T cell immunoglobulin and mucin protein-3 (Tim-3)/Galectin-9 interaction regulates influenza A virus-specific humoral and CD8 T-cell responses

Shalini Sharma[a], Aarthi Sundararajan[b], Amol Suryawanshi[a], Naveen Kumar[c], Tamara Veiga-Parga[a], Vijay K. Kuchroo[d], Paul G. Thomas[e], Mark Y. Sangster[b], and Barry T. Rouse[a,1]

[a]Department of Pathobiology, College of Veterinary Medicine, University of Tennessee, Knoxville, TN 37996-0845; [b]David H. Smith Centre for Vaccine Biology and Immunology, Department of Microbiology and Immunology, University of Rochester Medical Center, Rochester, NY 14642; [c]Department of Pathology and Laboratory Medicine, Emory University School of Medicine, Atlanta, GA 30322; [d]Center for Neurologic Diseases, Brigham and Women's Hospital and Harvard Medical School, Boston, MA 02115; and [e]Department of Immunology, St. Jude Children's Research Hospital, Memphis, TN, 38105-3678

Reactions to pathogens are usually tuned to effect immunity and limit tissue damage. Several host counterinflammatory mechanisms inhibit tissue damage but these may also act to constrain the effectiveness of immunity to acute infections, as we demonstrate in mice acutely infected with influenza A virus (IAV). We show that compared with wild type (WT), galectin-9 knockout (G9KO) mice mounted a more robust acute phase virus-specific CD8 T-cell response as well as higher and more rapid virus-specific serum IgM, IgG, and IgA responses and also cleared virus more rapidly than did WT mice. Blocking galectin-9 signals to Tim-3–expressing cells using a Tim-3 fusion protein resulted in improved immune responses in WT mice. When IAV immune mice were challenged with a heterologous IAV, the secondary IAV-specific CD8 T-cell responses were four- to fivefold higher in G9KO compared with WT mice. Our results indicate that manipulating galectin signals may represent a convenient approach to improve immune responses to some vaccines.

The host immune response to pathogens needs precise regulation to minimize tissue damage while still achieving defense (1, 2). Some bystander tissue damage usually happens because several host defenses can destroy cells or orchestrate inflammatory reactions. With chronic infections, for example, immune-mediated tissue damage would be more severe were it not for several cellular and chemical host components that inhibit inflammatory reactions (1). However, the activity of some of these counterinflammatory mechanisms could act to constrain the efficiency of protective immune components (3). For instance, regulatory T cells (Tregs) can inhibit inflammatory reactions associated with chronic virus infections (4), but the same Treg response can also limit the magnitude of protective immunity to a virus or induced by a vaccine (5, 6). Other host components may also function to limit and help resolve inflammatory reactions. These include some cytokines (7), groups of molecules derived from omega-3 polyunsaturated fatty acids (8), as well as some of the carbohydrate binding proteins of the galectin family (9). Galectin-9 (Gal-9), for example, upon binding to Tim-3 on T cells acts to limit the extent of immunopathological lesions in autoimmunity (10) as well as in some chronic infections (11–13). In the present study, we investigated whether the inhibitory effects of Gal-9 on Tim-3–expressing cells could influence the outcome of acute infection with influenza A virus (IAV). We demonstrate that animals lacking the regulatory effects of Gal-9/Tim-3 triggering mounted superior CD8 T-cell and humoral immune responses and they were more refractory to IAV. Moreover, IAV immune G9KO mice challenged with a heterologous IAV strain generated better virus-specific memory CD8 T-cell responses than WT animals. Our results indicate that manipulating galectin signaling may represent a convenient approach to improve responses to some vaccines.

Results

Virus-Specific CD8 T cells Up-Regulate Tim-3 Expression after IAV Infection.
Both bronchoalveolar lavage (BAL) and spleens were isolated at different times from IAV-infected wild-type (WT) animals and analyzed by FACS for CD8 T cells that expressed Tim-3. The highest levels in the BAL were observed at day 8, with 30–40% of total CD8 T cells expressing Tim-3 (Fig. 1A). In addition, most of these Tim-3^{+} cells were also CD44^{hi} and CD62L^{lo} (Fig. S1B, Upper) indicative of activated or effector phenotype. Peak frequencies of Tim-3^{+} CD8 T cells were also present on day 10 postinfection (p.i.) in the spleen (Fig. 2J). Using tetramers and the intracellular cytokine staining (ICCS) assay to detect D[b]NP$_{366-374}$ (ASNENMETM)-specific CD8 T cells, up to 75% IAV nucleoprotein (NP) tetramer-specific cells were Tim-3^{+} (Fig. 1 A and B) as well as CD44^{hi} and CD62L^{lo} (Fig. S1B, Lower). Furthermore, after NP peptide stimulation, the majority (around 75%) of IFNγ^{+} CD8 T cells were Tim-3^{+} (Fig. S1A). Endogenous levels of Gal-9 in the lung extracts of IAV-infected animals were also quantified by both Western blotting (Fig. S1C) and ELISA (Fig. S1D). Basal levels of Gal-9 were detectable in control lung extracts and these were moderately increased after IAV infection. A significant increase (2–2.5 fold) was observed at around 7 d p.i.

We could also show at day 10 p.i. that 20–22% of total CD4 T cells (Fig. 1C) were Tim-3^{+} in the BAL samples of the WT animals. Moreover, using the ICCS assay to detect NP311–325 (QVYSLIRPNENPAHK) peptide-specific CD4 T cells, up to 65–70% (on average) of virus-specific IFNγ^{+} CD4 T cells were Tim-3^{+} (Fig. 1D). Tim-3 expression was not detected on CD3^{−}B220^{+}CD19^{+} B cells.

Gal-9 Induces Apoptosis of IAV NPtet^{+}CD8 T Cells ex Vivo.
Ex vivo experiments were performed with splenocytes from IAV-infected mice at day 10 p.i. to determine whether the NPtet[+] population (the majority of which were Tim-3^{+}) would undergo apoptosis upon exposure to recombinant Gal-9. As shown in Fig. S2 B and D at an optimal dose the majority of NPtet[+] CD8 T cells became annexin V[+], indicative of their undergoing apoptosis, an effect inhibited by adding an excess of α-lactose (Fig. S2 A and B, Lower), the sugar that binds to Gal-9 and reduces its binding to Tim-3 (14, 15). The major effect of Gal-9 was observed in Tim-3^{+} cells (Fig. S3D) and was dose dependent. However, there was a low level of apoptosis of Tim-3^{−} cells (Fig. S3E) consistent with recent reports that Gal-9 could regulate T-cell function independently of Tim-3 (16). Our ex vivo results indicate that Gal-9 binding to Tim-3^{+} effectors causes them to die by apoptosis in vitro, an effect that might similarly occur in vivo.

Animals Unable to Produce Gal-9 Mount Better Acute-Phase Virus-Specific CD8 T-Cell Responses.
We reasoned that if the presence of endogenous Gal-9 acts to limit the magnitude of CD8 T-cell

IMMUNOLOGY

Fig. 1. Tim-3 expression is up-regulated on virus-specific CD8 T cells after IAV infection: At different time points after infection, BAL and spleen cells ($n = 3$) isolated at each time point were analyzed flow cytometrically for Tim-3 expression on IAV-specific CD8 T cells. BAL samples from three mice were pooled. (*A*) Percentage of total CD8 T cells and NPtet$^+$ CD8 T cells expressing Tim-3 in BAL is shown. (*B*) Frequencies of Tim-3$^+$ NPtet$^+$ CD8 T cells in the BAL of IAV-infected animals. (*C*) Histograms depict Tim-3 expression on CD4 T cells in WT and G9KO animals at day 10 p.i. in the BAL. (*D*) Representative FACS plots showing IFN$^+$ Tim-3$^+$ CD4 T cells in BAL of WT and G9KO animals upon NP$_{311-325}$ peptide stimulation. Numbers in the quadrants indicate percent of each subset. Data are representative of three independent experiments.

responses in the WT animals, then mice unable to produce Gal-9 due to gene knockout (G9KO), should respond better than WT animals to IAV. To analyze this possibility, WT and G9KO animals were infected intranasally with 5,000 egg infective dose, 50% (EID$_{50}$) of IAV (×31) and the magnitude of CD8 T-cell responses were compared 6, 8, and 10 d later. As shown, the responses of virus-specific CD8 T cells in both BAL and spleen, as measured by tetramers (Fig. 2 *A–E*) and ICCS (Fig. 2 *H–J*) were significantly higher at multiple time points in the G9KO mice. In both WT and G9KO animals up to 70–73% IFNγ^+ CD8 T cells were Tim-3$^+$ (Fig. 2*I*). However, a higher proportion of Tim-3$^+$ and NPtet$^+$ T cells in G9KO were CD44^{hi} (Fig. 2 *K* and *L*) and CD62L^{lo} (Fig. 2 *M* and *N*), indicating that more virus-specific CD8 T cells in G9KO animals expressed the activation phenotype. We also evaluated and compared the mean fluorescence intensity (MFI) of IFNγ and coexpression of multiple cytokines, both indicative of high quality T cells (17). G9KO animals expressed significantly higher MFI of IFNγ compared with WT animals (Fig. 2*F*). Collectively our data indicates that G9KO animals have a 2.5- to 3.5-fold augmented IAV-specific CD8 T-cell responses and have a higher proportion of CD8 T cells with properties of high quality.

ICCS was also performed on the BAL fluid cells using NP$_{311-325}$ peptide stimulation (to detect IAV-specific CD4 T cells) at day 10 p.i. G9KO mice had two- to threefold higher frequencies of IFNγ^+ CD4 T (IAV-specific CD4 T) cells in the BAL compared with the WT (Fig. 1*D*). Additionally, around 39–40% of CD4 T cells were Tim-3$^+$ at day 10 p.i. in the BAL of G9KO (Fig. 1*C*) compared with only 18–20% in the WT mice. It is conceivable that better CD4 T-cell responses of G9KO mice play a role in maintaining higher CD8 T-cell responses and also provide help for antibody (Ab) responses (18). Additionally, compared with WT mice, G9KO animals had fewer Tregs both in the BAL (Fig. S4 *A–C*) and spleen (Fig. S4*D*) particularly that were Tim-3$^+$ and CD103$^+$ (Fig. S4 *E* and *F*).

Gal-9 Knockout Mice Generate a More Rapid IAV-Specific Humoral Response. WT and G9KO mice were also compared for their plasma virus-specific Ab responses. Plasma levels of virus-specific IgM and IgG were substantially higher in G9KO compared with WT mice on day 7 (Fig. 3 *A* and *B*), indicating a markedly more rapid Ab response in the G9KO mice. IgG levels remained significantly higher in G9KO mice for at least 2 wk after infection. The strong early Ab response in G9KO mice reflected enhanced production of both the IgG1 and IgG2c isotypes, but by day 14 only IgG2c remained significantly higher in G9KO mice (Fig. 3 *C* and *D*). To gain further insights into the B-cell response, Ab-secreting cells (Fig. 3 *J* and *K*) and germinal center B cells (Fig. 3 *L* and *M*) in the draining lymph node on day 8 after infection were identified by flow cytometry. The proportion of cells with the B220^{int} CD138$^+$ phenotype of Ab-secreting cells was significantly higher in G9KO mice, consistent with the higher level of circulating virus-specific Ab early in the response. Interestingly, the proportion of PNA$^+$

FAS$^+$ germinal center B cells was significantly higher in WT mice, raising the possibility that strong early Ab-secreting cell formation in G9KO mice was at the expense of entry of activated B cells into germinal center reactions.

Virus-specific Ab levels were measured in the BAL to evaluate the IgA response as well as Ab-mediated antiviral activity at the site of viral replication. There was a trend toward higher BAL levels of IgG and IgA in G9KO compared with WT mice on day 10, but differences were not quite significant (Fig. 3 *E* and *F*). An analysis of virus-specific serum Ab levels in G9KO and WT mice on day 8 after IAV PR8 infection demonstrated a much earlier response in the G9KO mice (Fig. 3 *G* and *H*), consistent with the result after ×31 infection.

Diminished Viral Titers and Enhanced Viral Clearance in Gal-9 Knockout Mice. To evaluate whether G9KO and WT mice differed in their effectiveness at clearing viral infection, animals were infected with 5,000 EID$_{50}$ of IAV (×31) intranasally and the lungs from the infected WT and G9KO mice ($n = 3$ per group at each time point) were collected at days 2, 4, 7, 8, and 9 p.i. to quantify IAV. Viral levels were similar in early lung homogenate samples but by day 7 p.i., levels in G9KO mice were significantly ($P < 0.05$) decreased compared with WT (Fig. 3*I*). G9KO mice cleared virus by day 8 p.i., but WT animals still possessed virus 9 d p.i. The results of viral clearance experiments clearly indicated that G9KO animals had more effective protective immunity to IAV. Susceptibility of G9KO mice to IAV Hong Kong (HK)×31 was also compared with WT mice by three different approaches: body weight loss (Fig. S5), neutrophil infiltration (Fig. S6), and lung histopathology (Fig. S7). Our data indicate that G9KO showed greater weight loss and significantly increased CD11b$^+$Ly6G$^+$ neutrophil infiltration at day 3 p.i. in the BAL following IAV infection. By histopathology no differences were observed at the lower viral doses, but at 5×10^7 EID$_{50}$ multifocal type II pneumocytic hyperplasia was observable in at least 50% of the G9KO mice.

Gal-9 Knockout Mice Develop More Robust Recall Responses to IAV Infection. To compare recall response to IAV, animals were primed with ×31 then challenged intranasally (i/n) 41 d later with the heterologous IAV strain PR8. The NPtet$^+$ CD8 T-cell responses were around four- to fivefold higher in the G9KO compared with WT animals in the BAL (Fig. 4 *A* and *D*) and spleen (Fig. 4 *E*, *H*, and *I*). Additionally G9KO mice had a fourfold greater proportion of NPtet$^+$ cells that were Tim-3$^+$ in the BAL (Fig. 4*C*) and spleen (Fig. 4*G*). More interestingly, when primary and secondary responses were compared, WT mice expressed two- to threefold higher frequencies of NPtet$^+$ CD8 T cells compared with the primary response, whereas in G9KO mice, the NPtet$^+$ T-cell frequencies were enhanced eightfold. Furthermore a significantly higher proportion of NPtet$^+$ CD8 T cells were CD62L^{lo} (fivefold higher) in BAL (Fig. 4*B*) and (ninefold higher) in the

Fig. 2. Gal-9 knockout animals mount stronger virus-specific CD8 T-cell responses in the acute phase. Virus-specific CD8 T-cell responses were compared among age- and sex-matched IAV-infected WT and G9KO animals at indicated time points p.i. Representative FACS plots show NPtet$^+$CD8 T cells from WT and G9KO animals in the BAL (*A*) and spleen (*B*). (*C*) Absolute numbers of NPtet$^+$ and IFNγ$^+$TNFα$^+$ CD8 T cells at day 10 p.i. in BAL. Bar diagram shows the frequencies (*D*) and absolute numbers (*E*) of NPtet$^+$ CD8 T cells in spleen. (*F*) MFI of cytokine IFNγ produced by CD8 T cells in BAL. (*G*) Histograms showing Tim-3 expression on total BAL CD8 T cells in WT (light line) and G9KO mice (darker line) at day 10 p.i. Representative FACS plots show the frequencies of influenza A peptide NP$_{366-374}$ (ASNENMETM) stimulated polyfunctional (IFNγ$^+$TNFα$^+$) CD8 T cells isolated from the BAL (*H*, *Upper*) and spleen (*H*, *Lower*) at day 10 p.i. of WT and G9KO animals. (*I*) Tim-3 expression by IFNγ$^+$CD8 T cells in WT and G9KO animals at day 10 p.i. following stimulation with NP$_{366-374}$ peptide. (*J*) Absolute numbers of Tim-3$^+$, IFNγ$^+$, IFNγ$^+$TNFα$^+$ CD8 T cells in the spleen at indicated time points p.i. Coexpression of Tim-3 and NPtet$^+$ with CD44 in BAL (*K*), spleen (*L*), and with CD62L in BAL (*M*) and spleen (*N*) at day 8 p.i. is shown in WT and G9KO animals by representative FACS plots. Data are representative of three independent experiments with three mice per group in each experiment. Error bars represent SEM.

spleens (Fig. 4*F*) of G9KO animals. Using the ICCS assay IFNγ$^+$TNFα$^+$ CD8 T cells in BAL (Fig. 4*J* and *K*) and spleen (Fig. 4*L*) in G9KO mice were increased over WT, indicative of larger and higher quality responses. The significantly higher proportion of CD62L^{lo} and Tim-3$^+$ IAV NP tetramer-specific CD8 T cells in the G9KO mice that followed secondary infection suggests that a

greater proportion of these cells were in an activated state in G9KO mice during recall responses. In an attempt to address the issue of whether G9KO CD8 T cells were intrinsically more responsive or being less inhibited in G9KO environment, adoptive transfer experiments were conducted (Fig. S8*A*). The accumulation of WT D^{b}NPtet$^+$ donor Thy1.1$^+$ CD8 T cells was significantly

IMMUNOLOGY

Fig. 3. Enhanced virus-specific antibody production in G9KO mice after influenza infection. (*A–F*) WT and G9KO mice were sampled on the indicated days after intranasal infection with influenza ×31. Plasma levels of virus-specific IgM (*A*), IgG (B), IgG1 (*C*), and IgG2c (*D*), and BAL levels of virus-specific IgG (*E*) and IgA (*F*) were measured by ELISA. Titers are expressed as the reciprocal of the endpoint dilution and are shown as mean ±SE for six to eight individual mice in each group. (*G* and *H*) Plasma levels of virus-specific IgM (*G*) and IgG (*H*) on day 8 after intranasal infection with influenza PR8. The mean ±SE is shown for six to eight individual mice in each group. Arrows indicate values below the level of assay sensitivity. (*I*) On indicated days postinfection, lungs from WT and G9KO mice were collected and assayed for influenza viral titer by viral plaque assay. Representative FACS plots (*J*) and bar graphs (*K*) depicting the frequencies of CD3⁻B220⁺CD138⁺ B cells in the MLN of WT and G9KO mice at day 8 (D8) p.i. Representative FACS plots (*L, Upper*) naive; (*L, Lower*) day 8 p.i. and bar graphs (*M*) showing CD3⁻B220⁺PNA⁺ FAS⁺ germinal center B cells in the mediastinal lymph node (MLN) of WT and G9KO mice.

greater in G9KO than WT recipient animals (Fig. S8 *G* and *H*), indicating that Gal-9/Tim-3 signaling is responsible for the observed T-cell phenotype. The reverse experiment, where WT or G9KO (Thy1.2) cells were transferred to WT (Thy1.1) animals resulted in no observed differences in expansion. Taken together, our results suggest that the Tim-3/Gal-9 interaction acts in normal animals to limit the magnitude and efficiency of recall CD8 T-cell responses.

In Vivo Blockade of Tim-3 Pathway Results in Augmented Primary IAV-Specific CD8 T-Cell Responses. Our results indicated that Gal-9 may be playing a role in vivo to limit the extent of antiviral CD8 T-cell responses. To further evaluate the regulatory effect of Tim-3/Gal-9 interaction, this pathway was inhibited in vivo with a Tim-3 fusion protein (Tim-3 Ig). Using tetramers and the ICCS assay to record virus-specific CD8 T-cell responses in the BAL and spleen, Tim-3 blockade resulted in ~1.6- to twofold higher frequencies and fourfold higher absolute numbers of NPtet⁺ and IFNγ⁺TNFα⁺ CD8 T cells in BAL (Fig. 5 *A* and *B*) and spleen (Fig. 5*E*) at day 10 p.i. The blockade also resulted in better viral control (Fig. 5*C*). Additionally a higher proportion of virus-specific CD8 T cells were CD62L^lo both in the BAL (Fig. 5*D*) and spleen (Fig. 5*F*) of Tim-3 Ig-treated mice. A similar phenotype was observed when the Tim-3 fusion protein administration was begun at day 4 p.i. (Fig. S9).

Discussion

The host response to pathogens is usually tuned to effect immunity and to minimize any bystander tissue damage resulting from the immune reaction to the invader (1). Tissue damage is limited by several counterinflammatory events that act to functionally inhibit or destroy damaging cells as occurs when Gal-9 binds to one of its receptors, Tim-3 (14). Counterinflammatory events benefit the host in some chronic inflammatory processes (10, 19), autoimmunity,

and some viral immunopathological lesions (11, 14) but, as we demonstrate in this report, Tim-3/Gal-9 interactions can also act to limit the effectiveness of immunity to acute infectious agents, such as influenza virus. Accordingly, we show that mice lacking the ability to produce Gal-9 because of gene knockout generate more robust antiviral T-cell responses, more rapid antibody responses, and control intranasal infection more effectively than WT animals. The more effective responses to IAV by G9KO animals was explained by the observation that virus-specific CD8 and CD4 T cells up-regulate Tim-3 early after infection, making them susceptible to apoptosis upon binding to Gal-9, as we demonstrated in ex vivo studies. G9KO animals also developed better recall responses to IAV and generated superior CD8 T-cell responses compared with WT upon heterologous IAV infection. Our results could mean that manipulating signals that are usually provided by Gal-9 could result in improved responses to influenza vaccines.

Our data indicate that decreased cellular responses observed in WT animals were likely the consequence of the elevated endogenous production of Gal-9 that occurred after infection, along with the fact that most of the responder T cells, both CD8 and CD4, up-regulated the Tim-3 receptor. This scenario would set the scene for T-cell apoptosis as demonstrated by our ex vivo studies. However, alternative events might also explain the better responses of G9KO animals compared with WT. For example, G9KO animals have lower numbers of FoxP3⁺ Tregs compared with WT. Such cells could be responsible for suppressing the magnitude of influenza-specific T-cell responses as some have reported (20), at least as a minor effect. In addition to the observance of two- to threefold higher responses in G9KO animals, on the basis of multicytokine production and the levels of cytokine produced by antigen-stimulated CD8 T cells (17), the responses in G9KO mice were also of higher quality than were those in WT mice. This may mean that the levels of Tim-3 differ between responding T cells, accounting for differential suscep-
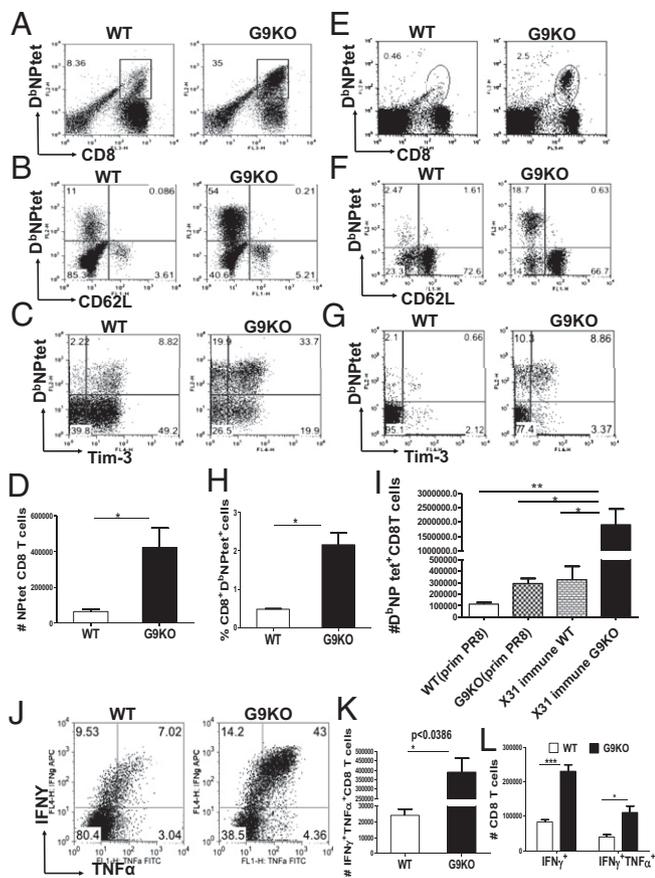
Fig. 4. Gal-9 knockout mice develop more robust recall responses to influenza A virus upon heterologous challenge. Both WT and Gal-9 KO animals primed 41 d previously with ×31 were challenged intranasally with 8,000 EID$_{50}$ of heterologous IAV (PR8) and the response in the BAL and spleen measured at day 8 postchallenge by tetramers and ICCS assays. Representative FACS plots showing the frequencies of NPtet$^+$ CD8 T cells in the ×31 immune WT and G9KO animals in BAL (A) and spleen (E and H), respectively. Absolute numbers of NPtet$^+$ CD8 T cells are shown in BAL (D) and spleen (I). Coexpression of NPtet and CD62L are shown in BAL (B) and spleen (F). Tim-3 expression on NPtet$^+$ CD8 T cells are isolated from BAL fluid (C) and spleen (G) of WT and G9KO animals. Representative FACS plots showing the frequencies (J) and absolute numbers (K) of IFNγ$^+$TNFα$^+$ CD8 T cells at day 8 postchallenge in the BAL of ×31 immune WT and G9KO animals. (L) Absolute numbers of IFNγ$^+$TNFα$^+$ CD8 T cells in the spleen of ×31 immune WT and G9KO animals. Data are representative of three independent experiments. Error bars represent SEM.

Fig. 5. Administration of Tim-3 fusion protein in mice after IAV infection enhances the magnitude and quality of IAV-specific CD8 T cell responses. IAV-infected C57BL/6 animals were treated with 100 µg of Tim-3 fusion protein per mice from day 1 postinfection at alternate days until day 9 p.i. and those in the other group were given control Ig and animals were killed at day 10 p.i. Percentages (A) and absolute numbers (B) of NPtet$^+$ and IFNγ$^+$ TNFα$^+$ CD8 T cells isolated from the BAL of Tim-3 fusion-protein treated and control animals are shown. (C) Viral titers in the lungs of control and Tim-3 Ig-treated mice. (D and F) Coexpression of NPtet and CD62L on CD8 T cells in BAL and spleen, respectively. (E) Absolute numbers of NPtet$^+$ CD8 T cells isolated from the spleen at day 10 p.i. Data are representative of three independent experiments with three to four mice per group. Error bars represent SEM.

tibility to Gal-9–mediated killing or inhibition. However, such effects were not formally investigated.

Whereas a number of previous studies reported the modulating effects of Tim-3/Gal-9 on T-cell–mediated lesions and immunity, few if any have analyzed the influence on Ab responses. We show that the early production of virus-specific antibody responses to influenza infection was strikingly enhanced in the absence of Gal-9. Because we could not demonstrate Tim-3 expression on B cells, their destruction as a consequence by Gal-9 binding would seem an unlikely mechanism. A better explanation may be that the enhanced responses of G9KO animals reflected the absence of modulating effects of Gal-9 on Tim-3–expressing helper CD4 T cells. Antibody responses to influenza virus are largely T cell dependent (21). Thus, accelerated B-cell help due to an increase in the availability or effectiveness of CD4 T cells could explain the stronger early antibody responses observed in G9KO mice (22, 23). We did not evaluate CD4 T-cell activation in lymph nodes draining the respiratory tract where cognate help for early B-cell responses is delivered. However, Gal-9 deficiency resulted in higher frequencies of virus-specific CD4 T cells in the airways after influenza infection, consistent with a more vigorous CD4 T-cell

response in the draining lymph nodes. The rapidity of the B-cell response in G9KO mice suggests an increase in antibody-secreting cell generation via the extrafollicular pathway of B-cell differentiation, an arm of the B-cell response that is enhanced by increased availability of T-cell help (24). The expression of Tim-3 by activated Th1 but not Th2 cells suggests that the Th1 response may be preferentially enhanced in G9KO mice. This could fit with the pattern of isotype expression in the antibody response of G9KO mice, because enhanced IgG2c production (driven by Th1-type cytokines) was sustained for longer than was IgG1 production (driven by Th2-type cytokines). We also observed that the frequency of germinal center B cells was significantly lower in G9KO than in WT mice, likely reflecting differentiation of activated B cells via the extrafollicular pathway at the expense of germinal center formation in G9KO mice. At this time, we cannot exclude other mechanisms that may also contribute to the enhanced Ab response in G9KO mice. For instance Gal-9 deficiency may limit other mechanisms of suppression (25), resulting in increased levels of factors that act directly on B cells to promote their activation (26).

Antiviral antibody production in response to influenza infection contributes in large part to viral control (27). We analyzed virus-specific antibody levels in the airways as a measure of antibody-mediated antiviral activity at the site of viral replication. This strategy also permitted an evaluation of the effect of Gal-9 deficiency on the virus-specific IgA response, because IgA-secreting cells generated in lymphoid tissues rapidly home to the respiratory tract submucosa and secretes IgA that is transported to the airway lumen (21, 28). IgG that is recovered from the airways is thought to be primarily derived from circulating anti-

IMMUNOLOGY

body by transduction (29). The levels of virus-specific IgG and IgA recovered from the airways on day 10 after infection were generally higher in G9KO compared with WT mice, but differences were not quite statistically significant. However, the overall kinetic pattern suggested earlier production of both IgG and IgA in G9KO mice and a contribution of these antibodies to antiviral activity in the lung during the phase of viral clearance. A strong IgA response in G9KO mice, as for the IgG response, may reflect a more vigorous and sustained CD4 T-cell response (21). However, this mechanism must be weighed against evidence that strong Th1 responses and IFNγ production, as might be expected in G9KO mice, are antagonistic to IgA production (30–32). Further studies are required to clarify this situation.

Materials and Methods

Mice and Virus Infections. Female 6–8-wk-old C57BL/6 were purchased from Harlan Laboratories and housed in the animal facilities at the University of Tennessee, Knoxville. G9KO were kindly provided by Gal Pharma. Stocks of IAV strains HK/×31 (H3N2)(×31) and A/Puerto Rico/8/34 (H1N1)(PR8) for mice infections were grown and titrated as described previously (33). Mice were infected intranasally with 5,000 EID_{50} of IAV HK×31 in 30-μl volume. To assess secondary CD8 T cell responses, mice were infected with ×31 and challenged intranasally at least 4 wk later with 8,000 EID_{50} of PR8. The animal care and use committee of the University of Tennessee approved all animal procedures.

Tissue Sampling. Spleen, BAL fluid, and plasma and lung samples were recovered from mice at acute phases of the primary and secondary infections. BAL samples were obtained from individual mice as described previously (34). Cells in the BAL were collected by centrifugation and the supernatants were stored at −80 °C for ELISA. BAL-associated cells were pooled from three mice in each group and single-cell suspensions were prepared from individual spleens. IAV ×31 titers in lungs were determined by plaque assay (35).

Tetramer and Phenotypic Staining of CD8 T Cells. Influenza A peptide $NP_{366-374}$ (ASNENMETM), $NP_{311-325}$ (QVYSLIRPNENPAHK) were kindly provided by the Trudeau Institute and John Altman (Emory University, Atlanta, GA), respectively. The experiments used the H-2D^b MHC class I glycoprotein complexed with the influenza virus NP ASNENMETM peptide (NP) and being designated NPtet and staining was done as described previously (36). H-2D^b-$NP_{366-374}$ is an immunodominant CD8 T-cell response to IAV in H-2b mice (37). ICCS assay was done as previously described (38).

ELISA. Virus-specific antibody levels in plasma and BAL were determined by ELISA using plates coated with purified, detergent-disrupted virus (21). The antibody titer is expressed as the reciprocal of the highest dilution giving an absorbance value more than twice that for simultaneously titrated samples from naive mice.

In Vivo Blockade and Virus Titrations. For blockade of Tim-3 pathway, 100 μg of Tim-3 Ig fusion protein was injected intraperitoneally on alternate days starting from day 1 until the time of sampling on day 10 p.i.

Statistical Analysis. Data were analyzed using Prism 5.0 software (GraphPad). Experiments were repeated two to three times. The data presenting the differences between the groups were assessed using two-tailed unpaired Student t tests or by two-way ANOVA with Bonferroni post hoc settings. ***$P < 0.001$, **$P < 0.01$, and *$P < 0.05$ were considered significant. $P < 0.05$ indicates that the value of the test sample was significantly different from that of relevant controls.

1. Rouse BT, Sehrawat S (2010) Immunity and immunopathology to viruses: What decides the outcome? *Nat Rev Immunol* 10:514–526.
2. Zinkernagel RM (1996) Immunology taught by viruses. *Science* 271:173–178.
3. Sehrawat S, et al. (2010) Galectin-9/TIM-3 interaction regulates virus-specific primary and memory CD8 T cell response. *PLoS Pathog* 6:e1000882.
4. Belkaid Y, Rouse BT (2005) Natural regulatory T cells in infectious disease. *Nat Immunol* 6:353–360.
5. Suvas S, Kumaraguru U, Pack CD, Lee S, Rouse BT (2003) CD4+CD25+ T cells regulate virus-specific primary and memory CD8+ T cell responses. *J Exp Med* 198:889–901.
6. Toka FN, Suvas S, Rouse BT (2004) CD4+ CD25+ T cells regulate vaccine-generated primary and memory CD8+ T-cell responses against herpes simplex virus type 1. *J Virol* 78:13082–13089.
7. Sun J, Madan R, Karp CL, Braciale TJ (2009) Effector T cells control lung inflammation during acute influenza virus infection by producing IL-10. *Nat Med* 15:277–284.
8. Serhan CN, Krishnamoorthy S, Recchiuti A, Chiang N (2011) Novel anti-inflammatory—pro-resolving mediators and their receptors. *Curr Top Med Chem* 11:629–647.
9. Rabinovich GA, Toscano MA (2009) Turning 'sweet' on immunity: Galectin-glycan interactions in immune tolerance and inflammation. *Nat Rev Immunol* 9:338–352.
10. Kuchroo VK, Meyers JH, Umetsu DT, DeKruyff RH (2006) TIM family of genes in immunity and tolerance. *Adv Immunol* 91:227–249.
11. Sehrawat S, Suryawanshi A, Hirashima M, Rouse BT (2009) Role of Tim-3/galectin-9 inhibitory interaction in viral-induced immunopathology: Shifting the balance toward regulators. *J Immunol* 182:3191–3201.
12. Golden-Mason L, et al. (2009) Negative immune regulator Tim-3 is overexpressed on T cells in hepatitis C virus infection and its blockade rescues dysfunctional CD4+ and CD8+ T cells. *J Virol* 83:9122–9130.
13. Jones RB, et al. (2008) Tim-3 expression defines a novel population of dysfunctional T cells with highly elevated frequencies in progressive HIV-1 infection. *J Exp Med* 205:2763–2779.
14. Zhu C, et al. (2005) The Tim-3 ligand galectin-9 negatively regulates T helper type 1 immunity. *Nat Immunol* 6:1245–1252.
15. Chabot S, et al. (2002) Regulation of galectin-9 expression and release in Jurkat T cell line cells. *Glycobiology* 12:111–118.
16. Su EW, Bi S, Kane LP (2010) Galectin-9 regulates T helper cell function independently of Tim-3. *Glycobiology* 21:1258–1265.
17. Seder RA, Darrah PA, Roederer M (2008) T-cell quality in memory and protection: Implications for vaccine design. *Nat Rev Immunol* 8:247–258.
18. Swain SL, Dutton RW, Woodland DL (2004) T cell responses to influenza virus infection: Effector and memory cells. *Viral Immunol* 17:197–209.
19. Kuchroo VK, Dardalhon V, Xiao S, Anderson AC (2008) New roles for TIM family members in immune regulation. *Nat Rev Immunol* 8:577–580.
20. Haeryfar SM, DiPaolo RJ, Tscharke DC, Bennink JR, Yewdell JW (2005) Regulatory T cells suppress CD8+ T cell responses induced by direct priming and cross-priming and moderate immunodominance disparities. *J Immunol* 174:3344–3351.
21. Sangster MY, et al. (2003) An early CD4+ T cell-dependent immunoglobulin A response to influenza infection in the absence of key cognate T-B interactions. *J Exp Med* 198:1011–1021.
22. Marshall D, Sealy R, Sangster M, Coleclough C (1999) TH cells primed during influenza virus infection provide help for qualitatively distinct antibody responses to subsequent immunization. *J Immunol* 163:4673–4682.
23. MacLeod MK, et al. (2011) Memory CD4 T cells that express CXCR5 provide accelerated help to B cells. *J Immunol* 186:2889–2896.
24. Rothaeusler K, Baumgarth N (2010) B-cell fate decisions following influenza virus infection. *Eur J Immunol* 40:366–377.
25. Dardalhon V, et al. (2010) Tim-3/galectin-9 pathway: Regulation of Th1 immunity through promotion of CD11b+Ly-6G+ myeloid cells. *J Immunol* 185:1383–1392.
26. Chang WL, et al. (2007) Influenza virus infection causes global respiratory tract B cell response modulation via innate immune signals. *J Immunol* 178:1457–1467.
27. Waffarn EE, Baumgarth N (2011) Protective B cell responses to flu—no fluke! *J Immunol* 186:3823–3829.
28. Joo HM, He Y, Sangster MY (2008) Broad dispersion and lung localization of virus-specific memory B cells induced by influenza pneumonia. *Proc Natl Acad Sci USA* 105:3485–3490.
29. Persson CG, et al. (1998) Contribution of plasma-derived molecules to mucosal immune defence, disease and repair in the airways. *Scand J Immunol* 47:302–313.
30. Ulloa L, Doody J, Massagué J (1999) Inhibition of transforming growth factor-beta/SMAD signalling by the interferon-gamma/STAT pathway. *Nature* 397:710–713.
31. Gajewski TF, Fitch FW (1988) Anti-proliferative effect of IFN-gamma in immune regulation. I. IFN-gamma inhibits the proliferation of Th2 but not Th1 murine helper T lymphocyte clones. *J Immunol* 140:4245–4252.
32. Cerutti A (2008) The regulation of IgA class switching. *Nat Rev Immunol* 8:421–434.
33. Joo HM, He Y, Sundararajan A, Huan L, Sangster MY (2010) Quantitative analysis of influenza virus-specific B cell memory generated by different routes of inactivated virus vaccination. *Vaccine* 28:2186–2194.
34. Nedrud JG, Liang XP, Hague N, Lamm ME (1987) Combined oral/nasal immunization protects mice from Sendai virus infection. *J Immunol* 139:3484–3492.
35. Kumar N, Xin ZT, Liang Y, Ly H, Liang Y (2008) NF-kappaB signaling differentially regulates influenza virus RNA synthesis. *J Virol* 82:9880–9889.
36. La Gruta NL, et al. (2010) Primary CTL response magnitude in mice is determined by the extent of naive T cell recruitment and subsequent clonal expansion. *J Clin Invest* 120:1885–1894.
37. Townsend AR, Bastin J, Gould K, Brownlee GG (1986) Cytotoxic T lymphocytes recognize influenza haemagglutinin that lacks a signal sequence. *Nature* 324:575–577.
38. Kumaraguru U, Rouse BT (2000) Application of the intracellular gamma interferon assay to recalculate the potency of CD8(+) T-cell responses to herpes simplex virus. *J Virol* 74:5709–5711.